International Journal of Solids and Structures 47 (2010) 2866–2871

Contents lists available at ScienceDirect

International Journal of Solids and Structures

journal homepage: www.elsevier.com/locate/ijsolstr

Discontinuity of quasi-static solution in the two-node Coulomb frictional system

Young Ju Ahn

Department of Mechanical Engineering, University of Michigan, Ann Arbor, MI 48109-2125, USA

ARTICLE INFO

Article history:
Received 3 September 2009
Received in revised form 11 April 2010
Available online 25 June 2010

Keywords:
Coulomb friction
Quasi-static problem
Discontinuity

ABSTRACT

A single-node system introduced by Klarbring has provided insight into the non-uniqueness of solution in the quasi-static contact problem at the high coefficient of Coulomb friction. Here, we explore this issue for the two-node system under the slip displacement space in which the instantaneous condition is efficiently represented. In the paper, we identify a qualitatively different failure of the quasi-static evolution algorithm in which a more complex dynamic transition may occur. When the system evolves from the point where both-node discontinuity occurs, the transient evolution behavior involving a damping matrix is explored in order to investigate a final state of the two-node system. It is demonstrated that the final state is uniquely determined which is independent of the damping matrix.

1. Introduction

Frictional contact systems comprising elastic bodies are common in engineering applications (Murthy et al., 2004; Law et al., 2006), and the governing equation of the interface behavior in such systems is frequently idealized by the classical Coulomb friction law. This simple approximation gives reasonable results compared to the experimentally observed behavior. However, it is well known that if the coefficient of friction is sufficiently high, problems of existence and uniqueness arise in both static and quasi-static problems. These problems in finite element method have been extensively studied by many authors (Janovský, 1980, 1981; Oden and Pires, 1983; Haslinger, 1983; Klarbring, 1987, 1990; Kikuchi and Oden, 1988), and the state of the art in these problems was reviewed by Andersson and Klarbring (2001). In particular, Klarbring (1990) explored this question in the context of a simple one-node system of two degree of freedom and demonstrated that three distinct quasi-static states, stick, separation and backward slip, are simultaneously possible for some loading scenarios if the coefficient of friction is higher than a critical value. In this case, the quasi-static problem may not determine a unique state solution. Further, Klarbring (1999) presented the generalized condition as Theorem 4 for which the rate problem has a unique solution in the analysis of the linear complementarity problems (LCPs).

This paper is concerned with the physical behavior of systems for which the coefficient of friction exceeds the critical value defined by Klarbring's criterion and for which therefore we may expect to encounter points in the loading scenario at which no combination of admissible nodal states (slip, stick, and separation) permits a solution satisfying the appropriate inequalities under the quasi-static assumption. For Klarbring's one-node system, Martins et al. (1994, 1995a) studied the nature of the quasi-static solution limit to a viscously damped dynamic solution by decreasing the mass and viscosity to zero. They showed that at the limit, multiple solutions are found and one of solutions, slip, may initiate snap-through jump for further evolution from the limit. Similarly, Cho and Barber (1998) developed the dynamic algorithm by adding inertia terms for the Klarbring's one-point model and compared the final states between the quasi-static and dynamic solutions. They showed that the state of backward slip in the quasi-static prediction is not possible in the dynamic analysis and results in a rapid state change to stick or separation, showing dynamic instability (Martins et al., 1995b; Adams, 1996). Using this finding, they proposed the revised quasi-static algorithm predicting instantaneous jump in position and state.

In this research, we consider the characteristic of a two-node system when the quasi-static solution reach the limit where the multiple solution exists. For the two-node system, it is not possible to effectively visualize multi-solution region in the external loading diagram used by Cho and Barber (1998). Instead, we would employ slip displacement space where the frictional inequalities define directional straight line constraints that tend to sweep the instantaneous slip condition as the external loading changes in time (Ahn et al., 2008; Barber and Ahn, 2009). This evolution mechanism could conveniently describe the possibility of a discontinuous transition at the two-node system depending on the magnitude of the coefficient of friction. In the slip displacement space, we shall explore the evolution behavior of the two-node system from the discontinuity point by using a perturbation analysis approach and examine the status changes. Thereafter, we shall verify that the unique final status can be predicted without a dynamic

E-mail address: yjahn@umich.edu

0020-7683/$ - see front matter © 2010 Elsevier Ltd. All rights reserved.
doi:10.1016/j.ijsolstr.2010.06.007

analysis, showing that a revised quasi-static algorithm is possible for the general loading.

2. The two-node coupled system with Coulomb friction law

We consider a two-dimensional two contacting node system illustrated in Fig. 1, in which each node is grounded by an elastic support and makes contact with a rigid frictional surface. Each node is also connected to each other by the coupling spring, implying that any tangential motion of each node generates normal component of reaction. We assume that an external loading $\boldsymbol{F}(\boldsymbol{t})$ is applied to the node and varies sufficiently slow for the quasi-static analysis is appropriate in which the reaction forces takes the form

$$q_j = q_j^w + A_{ji}v_i + B_{ij}w_i, \quad p_j = p_j^w + B_{ji}v_i + C_{ji}w_i \quad i,j = 1,2, \tag{1}$$

where v_i, w_i are, respectively, the tangential and normal displacements, q_i, p_i are the tangential and normal compressive nodal forces, q_i^w, p_i^w are the nodal reactions that would be generated by the external forces $\boldsymbol{F}(\boldsymbol{t})$ if all the nodal displacements were constrained to be zero and $\boldsymbol{A}$, $\boldsymbol{B}$, $\boldsymbol{C}$ are partitions of the reduced stiffness matrix $\boldsymbol{\kappa}$ (Klarbring et al., 2007). The coupling between tangential displacements and normal reactions is defined by the matrix $\boldsymbol{B}$.

2.1. The Coulomb friction law

The Coulomb friction law for node i can now be defined such that

$$w_i \geqslant 0\,; \quad p_i \geqslant 0, \tag{2}$$
$$w_i > 0 \;\Rightarrow\; p_i = q_i = 0, \tag{3}$$
$$p_i > 0 \;\Rightarrow\; w_i = 0, \tag{4}$$
$$|q_i| \leqslant fp_i, \tag{5}$$
$$|q_i| < fp_i \;\Rightarrow\; \dot{v}_i = 0, \tag{6}$$
$$0 < |q_i| = fp_i \;\Rightarrow\; \mathrm{sgn}(\dot{v}_i) = -\mathrm{sgn}(q_i), \tag{7}$$

where $f(>0)$ is the coefficient of friction and a superposed dot denotes the time derivative.

We suppose that at some point in the loading cycle both nodes are in contact, so that $w_1 = w_2 = 0$ and Eq. (1) reduces to

$$q_j = q_j^w + A_{ji}v_i; \quad p_j = p_j^w + B_{ji}v_i \quad i,j = 1,2. \tag{8}$$

Further, the inequality (5) at each node takes the form that

$$\begin{aligned}
&(A_{11} - fB_{11})v_1 + (A_{12} - fB_{12})v_2 \leqslant fp_1^w - q_1^w && \text{I},\\
&(A_{11} + fB_{11})v_1 + (A_{12} + fB_{12})v_2 \geqslant -fp_1^w - q_1^w && \text{II},\\
&(A_{21} - fB_{21})v_1 + (A_{22} - fB_{22})v_2 \leqslant fp_2^w - q_2^w && \text{III},\\
&(A_{21} + fB_{21})v_1 + (A_{22} + fB_{22})v_2 \geqslant -fp_2^w - q_2^w. && \text{IV}.
\end{aligned} \tag{9}$$

Each of the four inequalities I, II, III, and IV in Eq. (9) defines a straight line boundary in tangential displacement v_1, v_2 space and the region on one side of the line is admissible. As the external loading changes in time, four inequalities I, II, III, and IV moves in directions $\dot{v}_1 < 0, \dot{v}_1 > 0, \dot{v}_2 < 0, \dot{v}_2 > 0$, respectively. Notice that the location of the four constraint lines depends on the instantaneous values of q_i^w, p_i^w, but their slopes depend only on the matrices $\boldsymbol{A}$, $\boldsymbol{B}$ and the coefficient of friction f (Ahn et al., 2008).

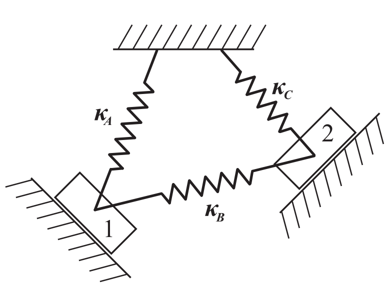

Fig. 1. The two contacting node model.

2.2. Single-node discontinuities in v_1, v_2 space

First, we consider the case where node 2 remains stuck and is strictly within the corresponding frictional bounds, whereas node 1 reaches the slip boundary defined by constraint I, as shown in Fig. 2.

This corresponds to the inequality

$$q_1 \leqslant fp_1 \tag{10}$$

and at the limit of equality we have

$$q_1 = fp_1 \tag{11}$$

for which the flow rule from Eq. (7) is

$$\dot{v}_1 < 0. \tag{12}$$

Thus, when the constraint I reaches the operating point P, it must 'push' P to the left. This is possible if and only if the angle of inclination θ of the line I to the vertical is between $-\pi/2 < \theta < \pi/2$. The angle θ is positive provided it follows counter clockwise as shown in Fig. 2. The critical condition arises when

$$A_{11} \leqslant fB_{11} \tag{13}$$

in Eq. (9).

For $A_{11} > fB_{11}$, regions on the right of the constraint line correspond to larger values of the left hand side of I in Eq. (9) and hence are inadmissible, whereas regions to the left are admissible. Thus, motion of v_1 in the correct slip direction ($\dot{v}_1 < 0$) takes P further into the admissible region. By contrast, for $A_{11} < fB_{11}$, regions to the left of the constraint line are inadmissible and hence no slip motion in the direction allowed by the flow rule is possible. The only remaining possibility is for the node to separate discontinuously since the reactions immediately before this transition are non-zero. This behavior is exactly analogous with that exhibited by Klarbring's one-node model (Cho and Barber, 1998) and results in an unstable motion to a new state involving separation at the node. Therefore, we conclude that the critical coefficient of friction is

$$f_1 = \frac{A_{11}}{|B_{11}|}. \tag{14}$$

Similar arguments applied to constraints II, III, and IV yield four critical coefficients in two equal and opposite pairs:

$$f_1, f_2, f_3, f_4 = \pm\frac{A_{11}}{|B_{11}|}, \pm\frac{A_{22}}{|B_{22}|}. \tag{15}$$

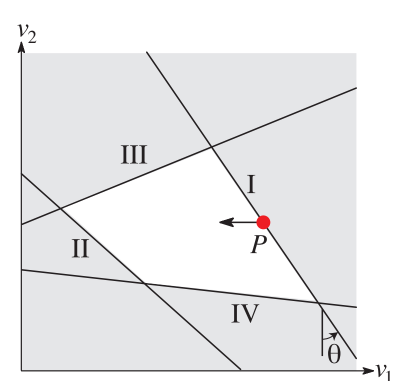

Fig. 2. Intersection of the admissible regions (white region) and motion of the instantaneous operating point P due to the advance of constraints I.

2.3. Two-node discontinuities in v_1, v_2 space

We suppose that the coefficient of friction satisfies the condition

$$f < min\{f_1, f_2, f_3, f_4\}, \tag{16}$$

so that in particular both constraints II and III are able to move the operating point in an admissible direction when operating independently. Suppose that once II becomes active, P will be moved to the right ($\dot{v}_1 > 0$) so as to stay on II until a situation is reached where P is at the intersection of II and III, as shown in Fig. 3. Further advance of II or III is now impossible, since the only admissible motion is that with $\dot{v}_1 > 0, \dot{v}_2 < 0$ and this sector is excluded by the constraints. Therefore, a discontinuous transition is the only option. The limiting coefficient of friction here is that where II and III are parallel, so

$$\det\begin{pmatrix} (A_{11} + fB_{11}) & (A_{12} + fB_{12}) \\ (A_{21} - fB_{21}) & (A_{22} - fB_{22}) \end{pmatrix} = 0 \tag{17}$$

or

$$A_{11}A_{22} - A_{12}A_{21} + (A_{22}B_{11} - A_{11}B_{22} + A_{12}B_{21} - A_{21}B_{12})f \\ - (B_{11}B_{22} + B_{12}B_{21})f^2 = 0; \tag{18}$$

which defines two critical values of f. Notice that we need to impose an additional condition for this state to hold. Since II excludes the region to the left and III excludes that to the top, an admissible region between them will occur if and only if both lines slope upwards to the left and hence

$$A_{22} - fB_{22} > 0, \tag{19}$$

since we have already imposed $A_{11} + fB_{11} > 0$ in requiring the constraint on f to be active. The corresponding condition where I and IV are parallel leads to identical equations except that f is replaced by $-f$. Additional conditions of the same kind can be obtained using the pairs I, III and II, IV. In each case, constraints must be imposed to ensure that the limiting case contains an admissible region, i.e., $A_{11} - fB_{11} > 0$ and $A_{22} - fB_{22} > 0$ in the pair I and III. Notice that the determinant criterion in (17) is a special case of the P-matrix condition in Klarbring's criterion (1999) which can generalize to the N-node system.

2.4. Wedging in v_1, v_2 space

Fig. 4, where the admissible region defined by all boundary constraints is open to infinity, shows that the system can become wedged (Ahn et al., 2008). In this case, multiple solutions always exist and discontinuous displacement jump occurs for some loading scenarios (Hassani et al., 2003; Barber and Hild, 2006). For example, constraint II in Fig. 4 advances until the only admissible region is an open triangle defined by II and III. This is the same situation as the two-node discontinuity described in Section 2.3. Therefore, if a two-node system is capable of being wedged, a two-node discontinuity is always possible. However, at this point, we need more investigation whether wedging is a necessary condition for a two-node discontinuity.

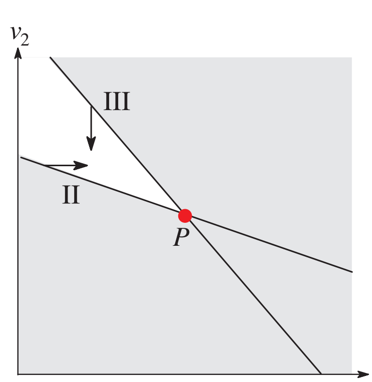

Fig. 3. Configurations of a two-node discontinuity.

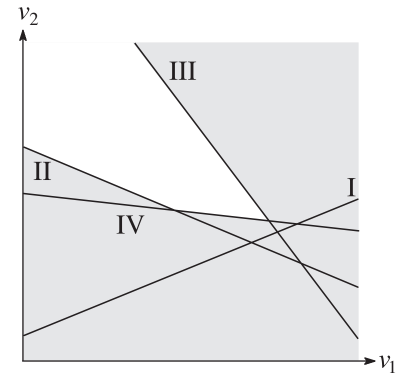

Fig. 4. Configurations of the constraints leading to wedging.

3. Perturbation analysis involving viscous damping

For the case where two-node discontinuity occurs, conditions (2)–(7) may fail to define a unique quasi-static evolution, and a more complex discontinuous transition may occur to a state involving one or both of the nodes separating. In the present paper, we shall examine the behavior of each node by using a transient algorithm involving a damping matrix and trace the change in status and displacement at each node.

3.1. Stability in the dynamic analysis

We first examine whether a quasi-static evolution is stable with a viscosity term if we are not at a discontinuity point. We suppose that an operating point is located on the slip boundary at node 1 defined by constraint I ($\dot{v}_1 < 0$), remaining node 2 stuck, which yields

$$(A_{11} - fB_{11})v_1^* + (A_{12} - fB_{12})v_2^* + q_1^w - fp_1^w = 0, \tag{20}$$

where v_1^*, v_2^* represent the equilibrium values at the moment.

We now wish to examine whether a small perturbation on this equilibrium point can grow or not when the constraint I advances, i.e., $\dot{v}_1 < 0$ and $\dot{v}_2 = 0$. By considering a small displacement perturbation δ on the equilibrium point, Eq. (20) including a damping term can be written as

$$D\dot{v}_1 + (A_{11} - fB_{11})v_1 + (A_{12} - fB_{12})v_2 + q_1^w - fp_1^w = 0, \tag{21}$$

where

$$v_1(t) = v_1^* + \delta v_1(t), \quad v_2(t) = v_2^*.$$

Here, D represents a positive damping coefficient.

Using Eqs. (20) and (21) reduces to

$$D\delta\dot{v}_1 + (A_{11} - fB_{11})\delta v_1 = 0. \tag{22}$$

The stability of the system depends on the homogenous solution in Eq. (22) that may grow or decay with time. The solution that contains one arbitrary constant a_1 can be written as

$$\delta v_1(t) = a_1 e^{-bt}, \tag{23}$$

where

$$b = \frac{A_{11} - fB_{11}}{D}.$$

Notice that the critical coefficient of friction, ($f = A_{11}/B_{11}$) is the same as that obtained in Eq. (14). If single node discontinuity does not occur in a system that satisfies the condition $A_{11} > fB_{11}$, the perturbation in Eq. (23) decays with time since b is a positive value. Hence, solution for a quasi-static evolution is always stable and is uniquely determined.

In comparison, we now suppose that a quasi-static evolution algorithm reaches the intersection point at (v_1^*, v_2^*) for the case where both constraint II and III are unable to move further, as shown in Fig. 3, yielding

$$(A_{11} + fB_{11})v_1^* + (A_{12} + fB_{12})v_2^* + q_1^w + fp_1^w = 0, \tag{24}$$

$$(A_{21} - fB_{21})v_1^* + (A_{22} - fB_{22})v_2^* + q_2^w - fp_2^w = 0, \tag{25}$$

where (v_1^*, v_2^*) can be obtained by solving Eqs. (24) and (25) simultaneously, assuming that the stiffness matrix, friction coefficient and external loadings, $\boldsymbol{r}^w$, are determined at a given evolution time, τ. At the point, a discontinuous transition is the only possible prediction. However, we may distinguish two different cases: (1) where both nodes are separated, or (2) one node is separated. The distinction depends on the external loading, $\boldsymbol{r}^w$.

3.2. Both nodes separated after discontinuity point

Firstly, if both nodes are separated, reaction forces along the contact area must be zero and the governing equation becomes

$$\{v_1, v_2, w_1, w_2\}^T = -\boldsymbol{\kappa}^{-1}\{q_1^w, q_2^w, p_1^w, p_2^w\}^T. \tag{26}$$

Since normal displacement at both nodes must be positive, i.e., $w_1 > 0$ and $w_2 > 0$, two inequality equations obtained from Eq. (26) constrain the feasible region of external loadings, $\boldsymbol{r}^w$. We can also define the feasible region of external loadings for the case where two-nodes discontinuity occurs, as in Eqs. (24) and (25). Hence, if an overlap area exists between two feasible regions, these external loadings in the overlapped region make the two separate at the discontinuity point.

3.3. One node separated after discontinuity point

Secondly, to resolve the case where external loadings do not make the two separate, we introduce a viscous damping matrix into the original quasi-static equation, yielding

$$\{q_1, q_2, p_1, p_2\}^T = \{q_1^w, q_2^w, p_1^w, p_2^w\}^T + \boldsymbol{\kappa}\{v_1, v_2, w_1, w_2\}^T + \boldsymbol{D}\{\dot{v}_1, \dot{v}_2, \dot{w}_1, \dot{w}_2\}^T, \tag{27}$$

where $\boldsymbol{D}$ is a 4 by 4 damping matrix consisting of diagonal damping coefficient terms, D_{ii} ($i = 1 \sim 4$).

We now wish to see whether a small perturbation at the discontinuity point, (v_1^*, v_2^*), can grow or decay in the transient dynamic time scale, t, which should be distinct from the quasi-static evolution time scale, τ. Note that the dynamic time scale, t, is considered to be much faster than the time in the quasi-static algorithm.

For giving an infinitesimal perturbation, there are three possible scenarios, i.e.,

(i) Node 1 is stick ($\delta\dot{v}_1 = 0$) and node 2 is backward slip ($\delta\dot{v}_2 < 0$),
(ii) Node 1 is forward slip ($\delta\dot{v}_1 > 0$) and node 2 is stick ($\delta\dot{v}_2 = 0$),
(iii) Node 1 is forward slip ($\delta\dot{v}_1 > 0$) and node 2 is backward slip ($\delta\dot{v}_2 < 0$).

Note that the first two cases could not give a meaningful result since the system always returns to the original discontinuity point because of its negative eigenvalue as described in Section 3.1. However, if the system is perturbed slightly at both nodes, as in the third case, the system will be unstable and depart from the discontinuity point. Hence, we will consider the behavior of only the third case.

3.3.1. Dynamic solution

Let

$$v_1(t) = v_1^* + \delta v_1(t), \quad v_2(t) = v_2^* + \delta v_2(t), \tag{28}$$

where δv_i represents a small perturbation for each node i. After taking the derivative of Eq. (3) with respect to time, t, the velocities $\dot{v}_1$ and $\dot{v}_2$ are written as

$$\dot{v}_1(t) = \delta\dot{v}_1(t), \quad \dot{v}_2(t) = \delta\dot{v}_2(t), \tag{29}$$

since v_1^* and v_2^* are both constants. Thus, by substituting Eqs. (3) and (29) into the inequalities II and III in Eq. (9), we can express these equations as

$$D_{11}\dot{v}_1 + (A_{11} + fB_{11})v_1 + (A_{12} + fB_{12})v_2 + q_1^w + fp_1^w = 0, \tag{30}$$

$$D_{33}\dot{v}_2 + (A_{21} - fB_{21})v_1 + (A_{22} - fB_{22})v_2 + q_2^w - fp_2^w = 0. \tag{31}$$

Further, Eqs. (30) and (31) reduce to the following homogeneous equations

$$D_{11}\delta\dot{v}_1 + (A_{11} + fB_{11})\delta v_1 + (A_{12} + fB_{12})\delta v_2 = 0, \tag{32}$$

$$D_{22}\delta\dot{v}_2 + (A_{21} - fB_{21})\delta v_1 + (A_{22} - fB_{22})\delta v_2 = 0, \tag{33}$$

since Eqs. (24) and (25) become zero at the discontinuity point, (v_1^*, v_2^*). The corresponding matrix equation is

$$\delta\dot{\boldsymbol{v}} = \boldsymbol{H}\delta\boldsymbol{v}. \tag{34}$$

where

$$\boldsymbol{H} = \begin{bmatrix} \frac{-(A_{11}+fB_{11})}{D_{11}} & \frac{-(A_{12}+fB_{12})}{D_{11}} \\ \frac{-(A_{21}-fB_{21})}{D_{22}} & \frac{-(A_{22}-fB_{22})}{D_{22}} \end{bmatrix}. \tag{35}$$

Hence, the disturbances δv_1 and δv_2 evolve in time, and the general solution for $\delta\boldsymbol{v}$ is

$$\delta\boldsymbol{v}(t) = a_1 e^{\lambda_1 t}\boldsymbol{\eta}_1 + a_2 e^{\lambda_2 t}\boldsymbol{\eta}_2. \tag{36}$$

where λ is an eigenvalue representing a growth rate, and $\boldsymbol{\eta}$ is an eigenvector with corresponding eigenvalue, λ. The λs can be found by the characteristic equation $det(\boldsymbol{H} - \lambda\boldsymbol{I}) = 0$, where $\boldsymbol{I}$ is the 2 by 2 identity matrix. The characteristic equation becomes

$$\det\begin{pmatrix} H_{11} - \lambda & H_{12} \\ H_{21} & H_{22} - \lambda \end{pmatrix} = 0. \tag{37}$$

Expanding the determinant yields

$$\lambda^2 - \alpha\lambda + \beta = 0 \tag{38}$$

where $\alpha = trace(\boldsymbol{H})$ and $\beta = det(\boldsymbol{H})$. Then,

$$\lambda_1 = \frac{\alpha - \sqrt{\alpha^2 - 4\beta}}{2}, \quad \lambda_2 = \frac{\alpha + \sqrt{\alpha^2 - 4\beta}}{2}. \tag{39}$$

From these equations, we can find the eigenvalues. Also, the general solution in Eq. (36) contains two arbitrary constants, a_1 and a_2, to enable us to satisfy initial conditions on $\delta\dot{v}_1(0)(>0)$ and $\delta\dot{v}_2(0)(<0)$ from the velocity equation

$$\delta\dot{\boldsymbol{v}}(t) = a_1\lambda_1 e^{\lambda_1 t}\boldsymbol{\eta}_1 + a_2\lambda_2 e^{\lambda_2 t}\boldsymbol{\eta}_2. \tag{40}$$

Suppose that the eigenvalues in Eq. (39) are real number, i.e., $\alpha^2 - 4\beta \geqslant 0$. Note that α is always negative value since we have already imposed $A_{11} - fB_{11} > 0$ and $A_{22} - fB_{22} > 0$ to avoid single node discontinuities. Therefore, λ_1 is always negative value, but the sign of λ_2 depends on the trace and determinant of the matrix $\boldsymbol{H}$. Especially, the limiting case, i.e., $\lambda_2 = 0$, occurs when $det(\boldsymbol{H}) = 0$, yielding

$$H_{11}H_{22} - H_{12}H_{21} = 0. \tag{41}$$

Note that the limiting condition in Eq. (41) is the same as that obtained in Eq. (17).

3.3.2. Unstable trajectory

When $det(\boldsymbol{H}) < 0$,λ_2 is a positive value, and an infinitesimal perturbation for $\delta\boldsymbol{v}$ will grow exponentially because of second term in Eq. (36) until normal reaction force at either nodes become zero at a given time, $t = t_1$, at which a state change occurs from slip to separation. The variation of normal reactions can be computed by the following equations:

$$p_1(t) = B_{11}\delta v_1 + B_{12}\delta v_2 + B_{11}v_1^* + B_{12}v_2^* + p_1^w, \tag{42}$$
$$p_2(t) = B_{21}\delta v_1 + B_{22}\delta v_2 + B_{21}v_1^* + B_{22}v_2^* + p_2^w. \tag{43}$$

Further, if we assume that normal reaction force at node 2 becomes zero earlier than at node 1, node 1 maintains forward slip state and node 2 changes from backward slip to separation state at $t = t_1$. Therefore, we need to set up the equations again that satisfy the Coulomb friction boundary conditions at both nodes. In order to find the system behavior for the time $t \geqslant t_1$, similar techniques can be used, as in the previous state. First, let

$$\{v_1(t),\ v_2(t),\ w_1(t),\ w_2(t)\}^T = \{v_1^* + \delta v_1(t),\ v_2^* + \delta v_2(t),\ \delta w_1(t),\ \delta w_2(t)\}^T. \tag{44}$$

Hence, the velocities are

$$\{\dot v_1(t),\ \dot v_2(t),\ \dot w_1(t),\ \dot w_2(t)\}^T = \{\delta\dot v_1(t),\ \delta\dot v_2(t),\ \delta\dot w_1(t),\ \delta\dot w_2(t)\}^T, \tag{45}$$

since v_1^* and v_2^* are both constants.

By applying friction boundary conditions at node 1 ($q_1 = -fp_1$, $\delta w_1(t) = 0, \delta\dot w_1(t) = 0$) and at node 2 ($q_2 = 0, p_2 = 0$), and by substituting Eq. (45) into Eq. (27), the following governing equation can be obtained

$$\begin{aligned} &D_{11}\delta\dot v_1 + (A_{11} + fB_{11})\delta v_1 + (A_{12} + fB_{12})\delta v_2 + (B_{21} + fC_{12})\delta w_2 + r_1^* = 0,\\ &D_{22}\delta\dot v_2 + A_{21}\delta v_1 + A_{22}\delta v_2 + B_{22}\delta w_2 + q_2^* = 0,\\ &D_{44}\delta\dot w_2 + B_{21}\delta v_1 + B_{22}\delta v_2 + B_{22}\delta w_2 + p_2^* = 0. \end{aligned} \tag{46}$$

where

$$\begin{aligned} r_1^* &= (A_{11} + fB_{11})v_1^* + (A_{12} + fB_{12})v_2^* + q_1^w + fp_1^w,\\ q_2^* &= A_{21}v_1^* + A_{22}v_2^* + q_2^w,\\ p_2^* &= B_{21}v_1^* + B_{22}v_2^* + p_2^w. \end{aligned} \tag{47}$$

Notice that r_1^* in Eq. (47) becomes zero from Eq. (24). These equations can be written in matrix form as

$$\delta\dot{\boldsymbol{x}} + \boldsymbol{G}\delta\boldsymbol{x} = \boldsymbol{P}^*, \tag{48}$$

where

$$\begin{aligned} \delta\boldsymbol{x} &= \{\delta v_1,\ \delta v_2,\ \delta w_2\}^T,\\ \delta\dot{\boldsymbol{x}} &= \{\delta\dot v_1,\ \delta\dot v_2,\ \delta\dot w_2\}^T,\\ \boldsymbol{G} &= \begin{bmatrix} \frac{A_{11}+fB_{11}}{D_{11}} & \frac{A_{12}+fB_{12}}{D_{11}} & \frac{B_{21}+fC_{12}}{D_{11}} \\ \frac{A_{21}}{D_{22}} & \frac{A_{22}}{D_{22}} & \frac{B_{22}}{D_{22}} \\ \frac{B_{21}}{D_{44}} & \frac{B_{22}}{D_{44}} & \frac{C_{22}}{D_{44}} \end{bmatrix},\\ \boldsymbol{P}^* &= \{0,\ -q_2^*/D_{22},\ -p_2^*/D_{44}\}^T. \end{aligned} \tag{49}$$

3.3.3. Final trajectory

The general solution, $\boldsymbol{g}$, for Eq. (48) can be written as the sum of a particular solution, $\boldsymbol{g}_P(t)$ and the homogeneous solution, $\boldsymbol{g}_H(t)$ which will contain three arbitrary constants to enable us to satisfy the following initial conditions:

$$\boldsymbol{g} = \boldsymbol{g}_H + \boldsymbol{g}_P, \quad \text{subjected to} \quad \delta\boldsymbol{x}(t_1) = \{\delta v_1(t_1),\ \delta v_2(t_1),\ 0\}^T. \tag{50}$$

By the characteristic equation $det(\boldsymbol{G} - \lambda\boldsymbol{I})$, three λ_s can be found, and the homogeneous solution in Eq. (50) is

$$\boldsymbol{g}_H = a_1 e^{\lambda_1 t}\boldsymbol{\eta}_1 + a_2 e^{\lambda_2 t}\boldsymbol{\eta}_2 + a_3 e^{\lambda_3 t}\boldsymbol{\eta}_3, \tag{51}$$

where $a_1 \sim a_3$ are arbitrary constants, $\lambda_1 \sim \lambda_3$ are eigenvalues, and $\boldsymbol{\eta}_1 \sim \boldsymbol{\eta}_3$ are eigenvectors corresponding to each λ.

If we assume that all λ_s are negative value, notice that the homogeneous solution, $\boldsymbol{g}_H$, becomes zero as $t \to \infty$ since all terms exponentially decay. Therefore, the general solution for Eq. (48) is determined by the following particular solution:

$$\boldsymbol{g} = \boldsymbol{g}_P = \boldsymbol{G}^{-1}\boldsymbol{P}^*, \tag{52}$$

where superscript -1 represents the matrix inverse. Furthermore, expanding the inverse matrix of $\boldsymbol{G}$ in Eq. (52) yields

$$\boldsymbol{G}^{-1} = \begin{bmatrix} G_{11}D_{11} & G_{21}D_{22} & G_{31}D_{44} \\ G_{21}D_{11} & G_{22}D_{22} & G_{32}D_{44} \\ G_{31}D_{11} & G_{23}D_{22} & G_{33}D_{44} \end{bmatrix}, \tag{53}$$

where each column includes the same damping coefficient, and the other coefficients are determined by the particular stiffness matrix and friction coefficient. By substituting Eq. (53) into Eq. (52), we can prove that the final state is not affected by the damping coefficients since these are canceled out by multiplication between $\boldsymbol{G}^{-1}$ and $\boldsymbol{P}^*$. Also, notice that since the vector, $\boldsymbol{P}^*$, is determined by particular values at the point that discontinuity occurs, it is possible for us to predict the final state of the system without involving the transient dynamic analysis.

4. Conclusions

For high coefficient of friction in a coupled system, we illustrated that the failure of the evolution in the slip displacement space can occur in which further advance of two boundary constraints is impossible, and its critical coefficient of friction for which the situation arise can be analytically defined by solving the two eigenvalue problems.

In a two-node discontinuity case, the transient numerical method involving a damping matrix was devised to track the dynamic trajectory satisfying the constraints. The dynamic trajectory showed that the final status is uniquely determined by the values at the discontinuity point without being influenced by the damping coefficients. Therefore, we would extract a matrix algebra algorithm that gets the final state from the initial state without having to solve the two eigenvalue problems. For multi-node system, a qualitatively different failure of the algorithm can occur in which the advance of two or more constraints each separately permit motion of the operating point in the appropriate direction, and we expect that a more complex dynamic transition occurs to a state involving one or more of the nodes separating. However, the finding obtained in the two-node system would be fruitful for further insight into the behavior of multi-node systems.

Acknowledgements

The author thanks Professor J.R. Barber for his sincere comment on these results.

References

Adams, G.G., 1996. Self-excited oscillations in sliding with a constant friction coefficient – a simple model. ASME Journal of Tribology 118, 819–823.

Ahn, Y.J., Bertocchi, E., Barber, J.R., 2008. Shakedown of coupled two-dimensional discrete frictional systems. Journal of the Mechanics and Physics of Solids 56, 3433–3440.

Andersson, L.-E., Klarbring, A., 2001. A review of the theory of static and quasi-static frictional contact problems in elasticity. Philosophical Transactions of the Royal Society of London 359, 2519–2539.

Barber, J.R., Ahn, Y.J., 2009. Discrete Coulomb frictional systems subjected to periodic loading. In: CMIS09, 5th Contact Mechanics International Symposium.

Barber, J.R., Hild, P., 2006. On wedged configurations with Coulomb friction. In: Peter Wriggers, Udo Nackenhorst (Eds.), Analysis and Simulation of Contact Problems. Springer-Verlag, Berlin, pp. 205–213.

Cho, H., Barber, J.R., 1998. Dynamic behavior and stability of simple frictional systems. Mathematical and Computer Modeling 28, 37–53.

Haslinger, J., 1983. Approximation of the signorini problem with friction, obeying the Coulomb law. Mathematical Methods in the Applied Science 5, 422–437.

Hassani, R., Hild, P., Ionescu, I.R., Sakki, N.-D., 2003. A mixed finite element method and solution multiplicity for Coulomb frictional contact. Computer Methods in Applied Mechanics and Engineering 192, 4517–4531.

Janovský, V., 1980. Catastrphic features of Coulomb friction model. Technical report KNM-0105044/80, Charles University, Prague.

Janovský, V., 1981. Catastrphic features of Coulomb friction model. In: Whiteman, J.R. (Ed.), The Mathematics of Finite Elements and Applications, pp. 259–264.

Kikuchi, N., Oden, J.T., 1988. Contact Problems in Elasticity: A Study of Variational Inequalities and Finite Element Methods. SIAM, Philadelphia.

Klarbring, A., 1987. Contact problems with friction by linear complementarity. In: Del Piero, G., Maceri, F. (Eds.), Unilateral Problems in Structural Analysis, vol. 2. Springer, pp. 197–219.

Klarbring, A., 1990. Examples of non-uniqueness and non-existence of solutions to quasi-static contact problems with friction. Ingenieur-Archiv 60, 529–541.

Klarbring, A., 1999. Contact, friction, discrete mechanical structures and mathematical programming. In: Wrigers, P., Panagiotopoulos, P. (Eds.), New Developments in Contact Problems. Springer, pp. 55–100.

Klarbring, A., Ciavarella, M., Barber, J.R., 2007. Shakedown in elastic contact problems with Coulomb friction. International Journal of Solids and Structures 44, 8355–8365.

Law, S.S., Wu, Z.M., Chan, S.L., 2006. Analytical model of a slotted bolted connection element and its behaviour under dynamic load. Journal of Sound and Vibration 292, 777–787.

Martins, J.A.C., Montiero Marques, M.D.P., Gastaldi, F., 1994. On an example of non-existence of solution to a quasistatic frictional contact problem. European Journal of Mechanics A/Solids 13, 113–133.

Martins, J.A.C., Simoes, F.M.F., Gastaldi, F., Monteiro Marques, M.D.P., 1995a. Dissipative graph solutions for a 2 degree-of-freedom quasistatic frictional contact problem. International Journal of Engineering Science 33, 1959–1986.

Martins, J.A.C., Guimaraes, J., Faria, L.O., 1995b. Dynamic surface solutions in linear elasticity and viscoelasticity with frictional boundary conditions. Journal of Vibration Acoustics 117, 445–451.

Murthy, H., Harish, G., Farris, T.N., 2004. Efficient modeling of fretting of blade/disk contacts including load history effects. ASME Journal of Tribology 126, 56–64.

Oden, J.T., Pires, E.B., 1983. Nonlocal and nonlinear friction laws and variational principles for contact problems in elasticity. ASME Journal of Applied Mechanics 50, 67–76.